EurJIC European Journal of Inorganic Chemistry

ChemPubSoc Europe

FULL PAPER

DOI:10.1002/ejic.201300576

Dinuclear Cu^{II}–Cu^{II} and Cu^{I}–Cu^{II} Complexes of a Compartmental Ligand – Syntheses, Structures, Magnetic, and Catalytic Studies

Surajit Biswas,[a] Arpan Dutta,[a] Malay Dolai,[a]
Indrani Bhowmick,[b,c] Mathieu Rouzières,[b,c] Hon Man Lee,[d]
Rodolphe Clérac,[b,c] and Mahammad Ali*[a]

Keywords: Schiff bases / Copper / Structure elucidation / Magnetic properties / Epoxidation

---

Dinuclear Cu^{II}–Cu^{II} (**1**) and Cu^{I}–Cu^{II} (**2**) complexes were derived from a new N_4O_2 donor compartmental ligand (H_2L) by changing the nature of the Cu precursors used. Single-crystal X-ray diffraction studies revealed that the Cu1 site in **1** has octahedral geometry and is in the inner compartment of the ligand axially coordinated by two ClO_4^- anions, whereas the outer Cu2 ion has square-pyramidal geometry. In **2**, there are two copper dinuclear complexes (A and B) in the asymmetric unit; the inner core is occupied by Cu1/Cu3 in the +2 oxidation state in a square-planar geometry. The Cu2/Cu4 ion occupies the outer sites and has distorted tetrahedral geometry with a +1 oxidation state. Complexes **1** and **2** were obtained simply by changing $Cu(ClO_4)_2$ in **1** to $Cu(ClO_4)_2$ and $Cu(bipy)(NO_3)_2$ in **2**; the bipyridyl (bipy) ligand induces the reduction of Cu^{II} to Cu^{I}, which is trapped in the Cu^{I}–Cu^{II} dinuclear product. The oxidation states of the metal ions were ascertained from charge-balance considerations as well as from bond valence sum (BVS) calculations. No signature of intervalence charge transfer (IVCT) was observed by spectroscopy (UV/Vis/NIR) as well as from the low-temperature magnetic studies. This might be because of the presence of two copper centers in two different geometries with a wide separation between them (ca. 3.27 Å). For **1**, the best fit of the χT vs. T data to the dimer model gives $J/k_B = -262(1)$ K and $g_{av} = 2.05(5)$, which indicates that there is a strong antiferromagnetic coupling between the two Cu atoms. In **2**, the Cu^{I} center is diamagnetic and, thus, the remaining $S = 1/2$ Cu^{II} magnetic center follows a Curie law with $g = 2.06(5)$. Under homogeneous conditions, both complexes showed catalytic epoxidation of cyclooctene, styrene, and norbornene to the corresponding epoxides with high selectivities and turnover numbers (TONs), which seem to be slightly better than the reported values for Cu^{II} Schiff base complexes.

Introduction

The synthesis and investigation of dinuclear complexes have attracted much attention because of their widespread application in the design of molecular materials (e.g., molecule-based magnets)[1] and as models for the active sites of many metalloproteins.[2] Many metalloenzymes such as hemocyanin (2Cu),[3] hemerythrin (2Fe),[4] tyrosinase (2Cu),[5] and methane monooxygenase (2Fe)[6] possess active sites with homodimetallic cores and involve either activation or transport of dioxygen in biological systems. Compounds containing metal atoms in two valence states are of special interest because of the possible electron transfer between these states;[7] this is the basic activity mechanism of many important chemical and biochemical catalytic reactions.[8] The most commonly studied mixed-valence transition-metal system incorporates Cu^{I}/Cu^{II} pairs because copper can adopt different coordination numbers and stereochemistry in its different oxidation states, which are both highly labile and stereochemically flexible[9,10] unlike other couples such as iron, cobalt, and ruthenium. Although a pronounced geometrical change is usually observed during the Cu^{I}/Cu^{II} interconversion, allosteric effects can also be observed.[11] Moreover, the control of the geometric environment around the copper centers allows the redox potential of the Cu^{I}/Cu^{II} couple to be tuned; this is the basis of the redox properties of type 1 copper proteins[12] and many synthetic analogues.[13,14] Nevertheless, it is very difficult to control the final product with two different oxidation states, which is reflected by the very limited number of reports on mixed-valence copper coordination compounds.[15–17]

On the other hand, compartmental ligands of the “end-off” type with a phenolic or alcoholic oxygen atom as an

---

[a] Department of Chemistry, Jadavpur University,
Kolkata 700 032, India
E-mail: m_ali2062@yahoo.com
Homepage: http://www.jaduniv.edu.in/profile.php?uid=30
[b] CNRS, CRPP, UPR 8641,
33600 Pessac, France
[c] Univ. Bordeaux, CRPP, UPR 8641,
33600 Pessac, France
[d] National Changhua University of Education, Department of Chemistry,
Changhua 50058, Taiwan

Supporting information for this article is available on the WWW under http://dx.doi.org/10.1002/ejic.201300576.

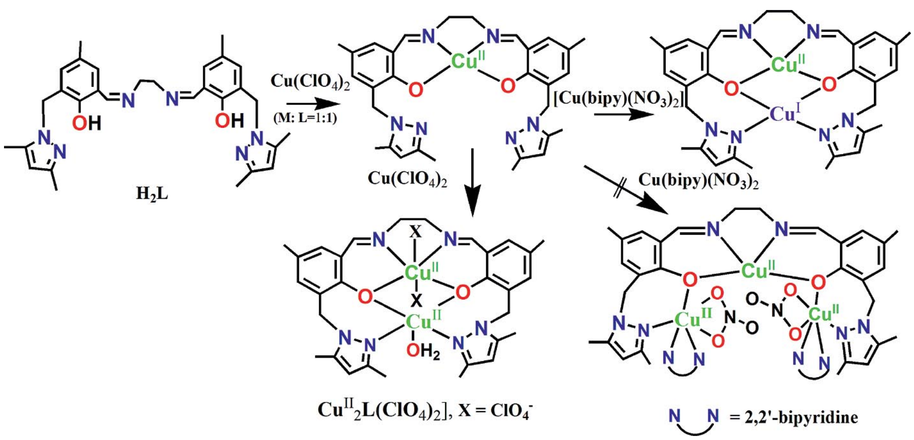

Scheme 1.

endogenous bridge are popular and often used to model dimetallic biosites. Indeed, they provide μ-phenoxido-μ-carboxylato and μ-phenoxido-di(μ-carboxylato) dinuclear cores that mimic the active sites of some dimetallic enzymes. Symmetric or asymmetric, cyclic or acyclic Schiff base ligands or their reduced analogues have generally been employed in these studies. The symmetric ligands are quite often prepared by one-step condensation of appropriately designed formyl or diformyl precursors. Moreover, epoxidation of olefins catalyzed by metal complexes has become an important research area in both organic synthesis and bioinorganic modeling of oxygen-transfer metalloenzymes.[18–24] For a variety of olefin substrates and oxygen-atom sources, good overall epoxidation is obtained with chiral Schiff base complexes of manganese(III) as catalysts,[18,19,25] which lead to significant enantiomeric excesses, more pronounced than those with the analogous manganese(II)[25] chromium(III),[26,27] and ruthenium(II/III) complexes.[19,28] In general, the oxygen-transfer processes mediated by the above-quoted complexes, and others such as iron(III), manganese(III), and chromium(III) porphyrins,[20] occur through the formation of high-valent metal oxido intermediates.[29,30] Although copper(II) Schiff base complexes have been known for more than 100 years, studies of their catalytic activities towards olefin epoxidation are rarely described.[31–33] We have already established that the H$_2$L ligand can form mononuclear LCu^{II} complexes (Scheme 1).[34] Herein, we report the synthesis and characterization of the dinuclear species LCu$^{II}_2$ (**1**) and LCu^{I}Cu^{II} (**2**) through single-crystal X-ray diffraction studies, magnetic-susceptibility measurements. Moreover, the catalytic activities towards the epoxidation of olefins, namely, cyclohexene, cyclooctene, and norbornene, by *tert*-butyl hydroperoxide (TBHP) were explored.

Results and Discussion

Structural Description

Single-crystal X-ray diffraction studies show that **1** crystallizes in the monoclinic $P2_1/c$ space group. In **1**, two Cu^{II} ions are coordinated by a N$_4$O$_2$ donor set of atoms from an L^{2-} ligand along with one water molecule (O10) and two perchlorate anions. The Cu1 ion is coordinated by two N atoms (N1 and N2) and two bridging phenoxido O atoms (O8 and O9) to form the equatorial plane; O1 and O7 from two perchlorate anions are coordinated in axial positions, and this leads roughly to an overall octahedral geometry around the Cu1 metal ion. The Cu1–O7 bond [2.852(2) Å] is significantly longer than the Cu1–O1 bond [2.504(2) Å] and, therefore, O7 can be considered as only semibonded to Cu1.[35] The two phenoxido O atoms are μ-bridges between the Cu1 and Cu2 ions. The two nitrogen atoms (N3 and N5) from the two appended pyrazole moieties and the two phenoxido oxygen atoms form the equatorial plane of the Cu2 site. Only one axial position is occupied by a water molecule (O10) to give a square-pyramidal geometry around the Cu2 ion. Hence, the geometries around the two Cu sites in the same asymmetric unit are different (Figure 1). The Cu1–Nx bond lengths (x = 1 and 2) are ca. 1.91 Å, whereas the Cu2–Nx (x = 3 and 4) bond lengths are ca. 1.97 Å (Table 1). The Cu1···Cu2 separation within the dinuclear unit is 3.002 Å. The μ-phenoxido bridges are not symmetrical and have different Cu–O bond lengths: the Cu1–O$_{\text{phenoxido}}$ and Cu2–O$_{\text{phenoxido}}$ bond lengths are

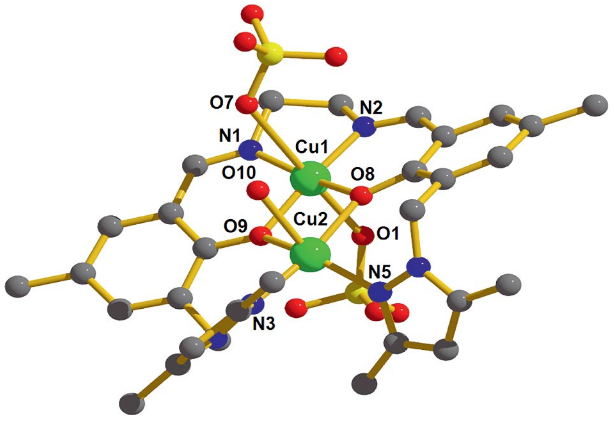

Figure 1. Molecular view of **1**. Color codes: green Cu^{II}, gray C, red O, blue N, yellow Cl. All H atoms are omitted for clarity.

1.936(1)/1.917(1) and 2.016(1)/2.055(1) Å, respectively. The slightly longer Cu–Ox (x = 8 and 9) bonds for Cu2 are likely the consequence of an imperfect match of the Cu2 ion size within the outer cavity. The displacement of Cu2 from the square plane constructed by O8, O9, N3 and N5 towards the axially coordinated water molecule by 0.194 Å induces the distorted square-pyramidal geometry. An inspection of supramolecular interactions present in the structure reveals that there are two strong H-bonding interactions between the coordinated water molecule and free perchlorate ions of the neighboring asymmetric unit and vice versa to give a H-bonded [O10–H1···O5 and O10–H1···O7] pair of dinuclear units (Figure 2).

Table 1. Selected bond lengths [Å] of **1** and **2**.

Bond lengths of **1**		Bond lengths of **2**	
Cu1–O1	2.5042(17)	Cu3–O1	1.906(5)
Cu1–O7	2.8523(16)	Cu3–O2	1.920(5)
Cu1–O8	1.9364(14)	Cu3–N7	1.932(7)
Cu1–O9	1.9171(14)	Cu3–N8	1.938(6)
Cu1–N1	1.9150(18)	Cu4–O1	2.336(5)
Cu1–N2	1.9122(18)	Cu4–O2	2.371(5)
Cu2–O8	2.0159(14)	Cu4–N9	1.906(7)
Cu2–O9	2.0548(14)	Cu4–N12	1.910(6)
Cu2–O10	2.2578(16)	Cu1–N2	1.935(8)
Cu2–N3	1.9740(18)	Cu1–N1	1.926(7)
Cu2–N5	1.9697(18)	Cu1–O3	1.908(5)
Cu1···Cu2	3.002	Cu1–O4	1.921(5)
		Cu2–O3	2.373(5)
		Cu2–O4	2.368(5)
		Cu2–N3	1.899(6)
		Cu2–N6	1.917(7)
		Cu1···Cu2	3.274
		Cu3···Cu4	3.261

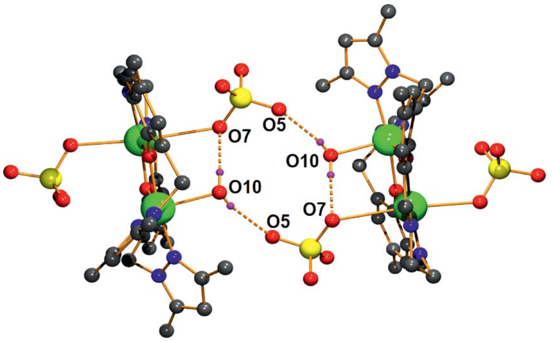

Figure 2. H-bonded supramolecular pairs of **1**. All hydrogen atoms are omitted for clarity [except those from the axially coordinated water molecules (O10), which are shown as pink spheres]. Bond lengths [Å] and angles [°] (D = donor, A = acceptor): D–H 0.690, H···A 2.260, D···A 2.937(2), ∠D–H···A 165.00 for O10–H1···O7; D–H 0.820, H···A 1.980, D···A 2.795(2), ∠D–H···A 174.00 for O10–H1···O5.

Complex **2** was obtained by reacting H_2L with $Cu^{II}(ClO_4)_2\cdot 6H_2O$ in a 1:1 molar ratio and then with $[Cu^{II}(bipy)(NO_3)_2]$ (bipy = 2,2′-bipyridine) in a 1:2 molar ratio in the presence of 2 equiv. triethylamine (TEA) with the motivation to synthesize a trinuclear complex $[LCu^{II}\{Cu(bipy)(NO_3)\}_2]^{2+}$. However, instead of $[LCu^{II}\{Cu(bipy)(NO_3)\}_2]^{2+}$, a mixed-valent dinuclear complex $LCu^{I}Cu^{II}$ (**2**) was formed in quantitative yield under reflux conditions.

There is a report on the kinetic and spectral studies on the autoreduction of Cu^{II} complexes of bipyridine and its derivatives under thermal conditions.[36] The 6,6′-dialkyl-2,2′-bipyridine (dmbp) Cu^{II} complex was automatically reduced in ethanol, whereas the bipy complex requires a reducing agent. Ultraviolet light[37,38] also reduces the Cu^{II} dmp complex in methanol. We have found that the reduction of Cu^{II} to form **2** in MeOH proceeds thermally without a reducing agent. This type of autoreduction of Cu^{II} complexes has also been found for a Cu^{II} complex of 8-dimethylarsinoquinoline.[39,40]

Single-crystal X-ray diffraction shows that **2** crystallizes in the triclinic $P\bar{1}$ space group. In **2**, the Cu^{II} and Cu^{I} ions are coordinated by N_4O_2 donor atoms from the deprotonated L^{2-} ligand. In the asymmetric unit, two crystallographically independent dinuclear units A and B are present. Both complexes display a very similar structure with subtle differences in bond lengths (Table 1) and angles (Table 2). Cu1 and Cu3 are coordinated by two N atoms (namely, N1 and N2 in A and N7 and N8 in B) of the ethylene diamine part of the ligand and two O atoms (O3 and O4 in A and O1 and O2 in B) from μ-phenoxido oxygen atoms, which also coordinate to the Cu2 and Cu4 metal ions, respectively, in the outer cavity. The geometry around the Cu1 and Cu3 sites is square planar. These Cu ions fit well within the ligand cavity with a very small displacement from the mean-square plane formed by N1, N2, O3, and O4 in A and N7, N8, O1, and O2 in B [0.030 Å for A and 0.028 Å for B]. On

Table 2. Selected bond angles [°] of **1** and **2**.

Bond angles of **1**		Bond angles of **2**	
O1–Cu1–O7	172.17(5)	O1–Cu3–O2	90.6(2)
O1–Cu1–O8	98.26(6)	O1–Cu3–N7	175.2(2)
O1–Cu1–O9	91.79(6)	O1–Cu3–N8	93.0(2)
O1–Cu1–N1	96.27(7)	O2–Cu3–N7	92.5(2)
O1–Cu1–N2	82.13(7)	O2–Cu3–N8	171.3(3)
O7–Cu1–O8	88.59(5)	N7–Cu3–N8	84.5(3)
O7–Cu1–O9	92.67(5)	O1–Cu4–O2	70.60(16)
O7–Cu1–N1	76.88(7)	O1–Cu4–N9	88.0(2)
O7–Cu1–N2	93.42(6)	O1–Cu4–N12	113.4(2)
O8–Cu1–O9	84.22(6)	O2–Cu4–N9	117.3(3)
O8–Cu1–N1	165.46(7)	O2–Cu4–N12	87.3(2)
O8–Cu1–N2	96.16(7)	N9–Cu4–N12	152.4(3)
O9–Cu1–N1	95.82(7)	N1–Cu1–N2	84.2(3)
O9–Cu1–N2	173.90(7)	O3–Cu1–N2	171.5(3)
N1–Cu1–N2	85.35(8)	O3–Cu1–O4	91.2(2)
O8–Cu2–O9	78.80(6)	O3–Cu1–N1	92.4(3)
O8–Cu2–O10	85.13(6)	O4–Cu1–N1	175.3(3)
O8–Cu2–N3	171.54(7)	O4–Cu1–N2	92.6(3)
O8–Cu2–N5	95.36(7)	O3–Cu2–O4	70.50(16)
O9–Cu2–O10	87.01(6)	O3–Cu2–N6	89.0(2)
O9–Cu2–N3	99.27(7)	O4–Cu2–N3	88.1(2)
O9–Cu2–N5	149.09(7)	O3–Cu2–N3	115.10(19)
O10–Cu2–N3	86.55(7)	N3–Cu2–N6	150.9(3)
O10–Cu2–N5	123.04(7)	O4–Cu2–N6	116.6(2)
N3–Cu2–N5	90.44(7)	Cu3–O1–Cu4	100.0(2)
Cu1–O8–Cu2	98.80(6)	Cu3–O2–Cu4	98.4(2)
Cu1–O9–Cu2	98.11(6)	Cu1–O3 –Cu2	99.2(2)
		Cu1–O4–Cu2	99.0(2)

the other hand, Cu2 and Cu4 are coordinated by two N atoms (namely, N6 and N3 in A and N12 and N9 in B) from the two pyrazole units of the ligand and two O atoms (O4 and O3 in A and O1 and O2 in B) from the phenolate oxygen atoms, which leads to a distorted tetrahedral geometry around the Cu2 and Cu4 centers (Figure 3). Their oxidation state is +I on the basis of charge balance, coordination geometry, and bond valence sum (BVS) calculations (Table S1).[41] Two perchlorate anions remain uncoordinated to satisfy the +2 charge of the complex in the asymmetric unit. The Cu···Cu separation within the dinuclear complexes is 3.274 Å in A and 3.261 Å in B.

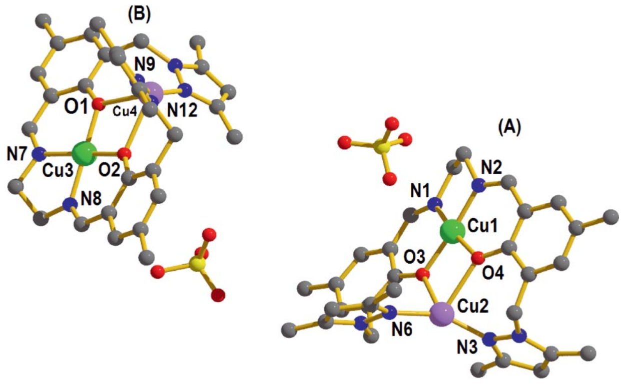

Figure 3. Molecular view of **2**. All H atoms are omitted for clarity. Color codes: green Cu^{II}, light violet Cu^{I}, gray C, red O, blue N, yellow Cl.

UV/Vis Spectra

The electronic spectra of **1** and **2** were recorded in MeCN (Figure 4). The electronic transition bands for **1** appear at 518 and 348 nm with molar extinction coefficients (ε) of 811.3 and 9.7×10^4 dm^{3}mol^{-1}cm^{-1}, respectively. The corresponding bands for **2** appear at 586 and 368 nm with ε values of 367.1 and 1.9×10^5 dm^{3}mol^{-1}cm^{-1}, respectively. The bands at longer wavelengths may be attributed to the d–d transitions, whereas bands at ca. 348 and 368 nm are likely due to metal-to-ligand charge-transfer transitions. UV/Vis/NIR studies did not provide any indication of intervalence charge transfer (IVCT), which indicates that the charges are localized on the two Cu centers. This is also supported by the low-temperature magnetic studies (vide infra).

Solvatochromism arises mainly because of the influence of the solvent on the electronic absorption and emission spectra of molecules. Among the solvatochromic metal complexes, the mixed-chelate copper(II) complexes have received great attention because the presence of a strong Jahn–Teller effect results in simple and regular changes in their electronic spectra according to the strength of interactions with solvent molecules at the axial sites.[42]

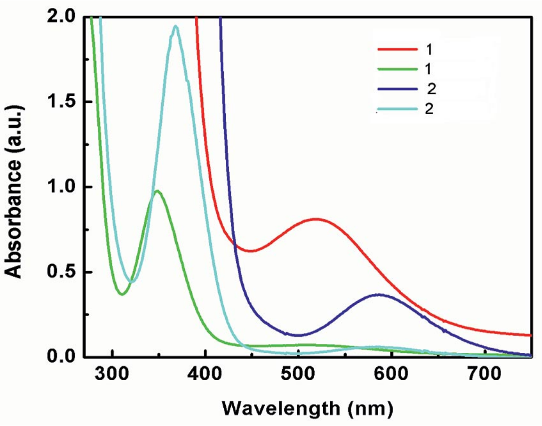

Figure 4. UV/Vis spectra of **1** and **2** in MeCN. [c] = 1.0×10^{-3} M for d–d bands at wavelengths above 450 nm and [c] = 1.0×10^{-5} M for MLCT bands at wavelengths below 400 nm.

Complex **1** is soluble in a wide range of organic solvents and demonstrates solvatochromic properties. As the electronic configuration of the copper(II) ion is d^9, the broad structureless absorption band is associated with the transition of the electron from the lower-energy orbitals to the hole in $d_{x^2-y^2}$ orbital, which is influenced by the solvent strength towards axial coordination. The visible spectral changes of these complexes in some selected solvents are illustrated in Figure 5. For **2**, no such solvatochromic behavior is apparent (inset Figure 5), maybe because the Cu^{II} ion is in a square-planar geometry and is quite reluctant to accommodate any solvent molecule axially.

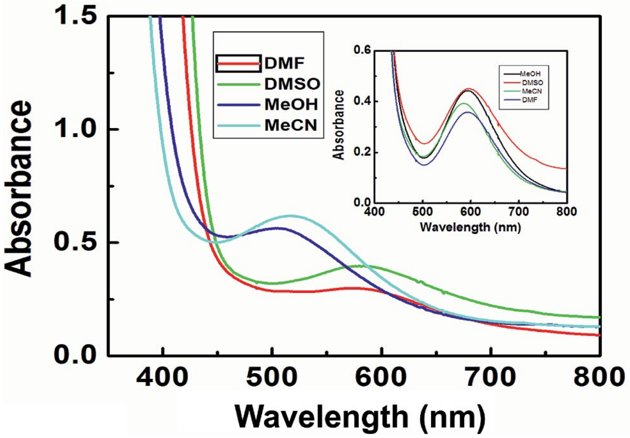

Figure 5. Absorption spectra of **1** in selected solvents. Inset is the absorption spectra of **2**.

Catalytic Activities

Olefin epoxidation reactions catalyzed by different transition-metal-based catalysts under homogeneous[43] and heterogeneous conditions[44–49] are well documented. The epoxidation of styrene by copper phthalocyanine immobilized on NaY under heterogeneous conditions showed over 95% conversion with epoxide selectivity of only ca. 24%.[44] MCM-41-anchored copper phthalocyanine has increased epoxide selectivity of ca. 53%; however, the conversion remains at ca. 47%.[45]

The epoxide selectivity of styrene epoxidation with *t*BuOOH as oxidant rarely goes above 40% under heterogeneous conditions with copper/copper complexes immobilized on zeolite or with molecular sieves.[45] Very recently, an MCM-41-anchored copper(II) Schiff base catalyst improved the styrene conversion to epoxide to ca. 86%.[31c] Rayati et al. studied the styrene epoxidation over two copper(II) Schiff base complexes under homogeneous conditions with *t*BuOOH, and over 95% conversion with an epoxide selectivity of only ca. 25% was obtained.[31b] Similar styrene epoxidation under homogeneous conditions with *t*BuOOH results in only 39–54% yield with selectivity of 39–72%.[31c,31d] Thus, although aromatic and aliphatic alkenes react with *t*BuOOH to produce the corresponding epoxides with only low-to-moderate selectivity when catalyzed by the Cu Schiff base complexes,[44–50] these complexes have been scarcely used as homogeneous catalysts in olefin oxidation reactions.[50,51] In the present report, we have explored the catalytic epoxidation of three olefins, namely, styrene, cyclooctene, and norbornene, by *t*BuOOH in the presence of a catalytic amount of Schiff base complexes **1** and **2** in MeCN (Scheme 2). The results of the catalytic oxidation of different substrates are given in Table 3. Under homogeneous conditions, the oxidation of styrene with *t*BuOOH gives styrene epoxide in ca. 52% yield (selectivity 76%) with a turnover number (TON) of ca. 270 (Table 4) along with a moderate amount of benzaldehyde (ca. 16%). Both complexes show almost similar selectivity and TON in the production of styrene epoxide. Das et al. have obtained a moderate yield of olefin epoxide by using a copper(II) Schiff base complex as a catalyst in the presence of 2-methylpropanal and molecular oxygen under homogeneous conditions,[50a] and a maximum yield of ca. 15% of styrene oxide has been achieved with iodosylbenzene and the same Schiff base copper complexes.[50b] The oxidation of cyclooctene by *t*BuOOH (Table 4) catalyzed by **1** and **2** proceeds smoothly and shows excellent conversion of 74–78%. Nevertheless, the desired product, cyclooctene oxide, was not the sole product of this reaction and was produced with moderate selectivity (ca. 60%). Apart from cyclooctene oxide, cyclooctane-1,2-diol (18%) was also generated owing to allylic C–H oxidation. The bulkier cycloalkene norbornene has been effectively converted to *exo*-epoxynorbornane (conversion 85–87%, selectivity 98%). Graphical representations of the relative efficiencies of the catalysts for different alkenes are given in Figures 6 and S1 for **1** and **2**, respectively.

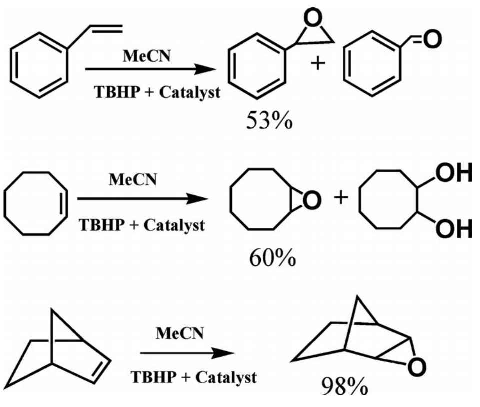

Scheme 2.

Table 3. Homogeneous catalytic oxidation of olefins by TBHP to epoxides catalyzed by **1** and **2** (catalyst concentration: 0.03 mmol).

Cat.	Substrate	Reaction time [h]	Conv. [%]	% Yield of products Epoxide	Others	TON
1	norbornene	24	87	85	02	348
	cyclooctene	24	78	60	18	312
	styrene	24	70	53	17	280
2	norbornene	24	85	81	04	340
	cyclooctene	24	74	57	17	296
	styrene	24	68	52	16	272

Table 4. Comparison of the catalytic efficiency of **1** and **2** with other reported copper(II) catalysts for the cyclohexene oxidation with *t*BuOOH in MeCN.

Catalyst[a]	Conv. [%]	Epoxide selectivity [%]	Ref.
$[Cu(L^1)(H_2O)](ClO_4)$	86	42	[31c]
$[Cu(L^2)]$	75	54	[31c]
$[Cu(L^3)]$	99	39	[31c]
$[Cu(HL^4)(NO_3)]$	62	64	[52]
$\{[Mg(H_2O)_6][Cu(pydca)\cdot 2H_2O]\}_n$	52	52	[52]
LCu^{II}_2 (**1**)	70	53	this work
$LCu^{I}Cu^{II}$ (**2**)	68	52	this work

[a] HL^1 = 1-(*N*-*ortho*-hydroxyacetophenimine)-2-methylpyridine; H_2L^2 = *N*,*N*′-(2-hydroxypropane-1,3-diyl)bis(salicylideneimine); H_2L^3 = *N*,*N*′-(2,2-dimethylpropan-1,3-diyl)bis(salicylideneimine); H_2L^4 = 1-(*N*-*ortho*-hydroxyacetophenimine)ethan-2-ol; H_2pydca = 2,5-pyridine dicarboxylic acid.

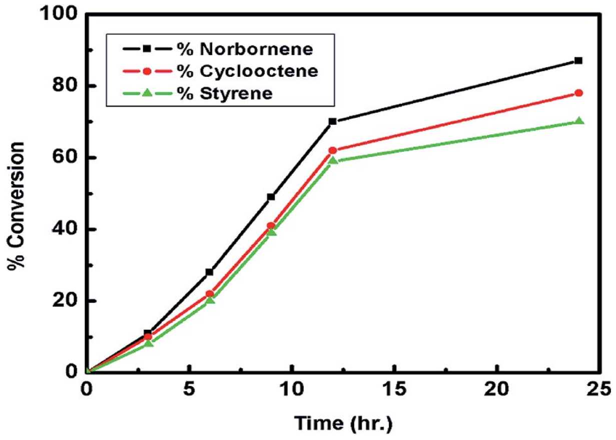

Figure 6. Conversions [%] of styrene (green), cyclooctene (red), and norbornene (black) at different reaction times in the liquid phase catalyzed by **1**.

The efficacy of the different catalysts in MeCN with *t*BuOOH as oxidant is summarized in Table 4. Interestingly, our dinuclear complexes lead to almost comparable conversions but with comparable/better selectivity under identical reaction conditions. Both complexes exhibit almost equal catalytic activities towards olefin epoxidation irrespective of the Cu oxidation state and complex geometry. More study is needed on this aspect in related systems before further speculation.

Magnetic properties

The temperature-dependent magnetic susceptibilities for **1** and **2** were measured at 1000 Oe direct current (dc) field between 1.8 and 300 K and are shown as χT vs. T plots (Figure 7). At 300 K, the χT product of **1** is 0.72 $cm^3\,K\,mol^{-1}$, which is lower than the theoretical value of 0.75 $cm^3\,K\,mol^{-1}$ expected for two isolated paramagnetic Cu^{II} ions (d^9, $S = 1/2$, $g = 2$). This result suggests the presence of antiferromagnetic interactions between the Cu^{II} ions within the dinuclear complex. Confirming this hypothesis, the χT product continuously decreases as the temperature decreases to reach a value close to zero below 50 K. As shown in the crystal structure analysis (vide supra), complex **1** can be viewed as a dinuclear $S = 1/2$ Cu^{II} unit. Thus, the magnetic data have been modeled by using the Heisenberg spin dimer Hamiltonian of isotropic $S = 1/2$ spins given by Equation (1).

$$H = -2JS_{Cu1}S_{Cu2} \qquad (1)$$

J is the magnetic interaction within the dinuclear Cu^{II} unit and S_i are the spin operators for each $S = 1/2$ center (Cu1 and Cu2).

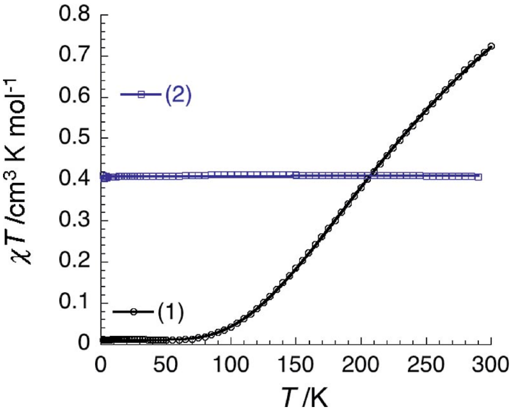

Figure 7. Temperature dependence of the χT product (χ is the molar magnetic susceptibility that equals M/H per complex) recorded in an applied dc magnetic field of 1000 Oe for **1** (black) and **2** (blue). The black circles and blue squares correspond to the experimental data for **1** and **2**, and the solid lines are the best fits obtained from a Heisenberg $S = 1/2$ spin dimer model and the Curie law, respectively (see text).

The application of the van Vleck equation[53] to the Kambe vector coupling scheme[54] allows determination of the low-field analytical expression of the magnetic susceptibility [Equation (2)].[55]

$$\chi T = \frac{2Ng^2\mu_B{}^2}{k_B}\,\frac{1}{3 + \exp(-2J/k_BT)} \qquad (2)$$

The best fit of the χT vs. T data (solid line in Figure 7) is obtained with $J/k_B = -262(1)$ K and $g_{av} = 2.05(5)$. This simple magnetic model is able to reproduce well the experimental χT vs. T data from 300 to 1.8 K. The sign of the magnetic interactions implies that this dinuclear Cu complex possess an $S_T = 0$ spin ground state as expected for similar di-alkoxido-bridged dinuclear Cu^{II} complexes.[1,56] As shown in Figure 7, the χT product of **2** at 290 K is 0.40 $cm^3\,K\,mol^{-1}$. This value corresponds to the theoretical one expected for one isolated $S = 1/2$ Cu^{II} center with $g = 2.06(5)$ associated with one diamagnetic Cu^I metal ion. As the temperature decreases, the χT product remains unchanged in magnitude until 1.8 K. Such thermal Curie-type paramagnetic behavior implies that the magnetic interactions between the $S = 1/2$ Cu^{II}/Cu^I mixed valence complexes are negligible above 1.8 K. Furthermore, the field dependence of the magnetization was measured at 1.83–8 K. At 1.83 K, the magnetization is almost saturated at 7 T to a value of 0.99 μ_B (Figure S2). As the Cu^{II} spin carriers in **2** are magnetically isolated, the M vs. H/T data at 1.83 K fit perfectly to an $S = 1/2$ Brillouin function (Figure S2) with a Landé factor of 2.05(3) in excellent agreement with the estimated value from the χT vs. T data (vide supra).

Conclusions

We have synthesized two new dinuclear complexes $LCu^{II}{}_2$ (**1**) and LCu^ICu^{II} (**2**) from a mononuclear LCu^{II} species of a new compartmental ligand H_2L. Both complexes have been characterized by spectroscopic techniques and single-crystal X-ray diffraction. In **1**, the Cu1 site is in an octahedral geometry positioned in the inner compartment of the L^{2-} ligand, whereas Cu2 occupies the outer compartment in a square-pyramidal geometry. In **2**, the inner core is occupied by a Cu^{II} metal ion in a square-planar geometry, whereas the outer site is filled by a Cu^I center in a distorted tetrahedral geometry. The modeling of the magnetic properties of **1** by a Heisenberg $S = 1/2$ dimer model allows us to quantify the large intracomplex antiferromagnetic interaction [–262(1) K] that is usually observed in this type of dinuclear Cu^{II} complexes. In **2**, the Cu^I ion is diamagnetic and, thus, its magnetic properties are dominated by the isolated Cu^{II} $S = 1/2$ spin center, which follows a simple Curie law. Under homogeneous conditions, both complexes showed catalytic epoxidation of cyclooctene, styrene, and norbornene to the corresponding epoxides with high selectivities and TONs, which appear to be higher than the reported values for other Cu^{II} Schiff base complexes.

Experimental Section

Reagents: 2-(Chloromethyl)-6-formyl-4-methylphenol, 3,5-dimethylpyrazole, and $[Cu(2,2'\text{-bipy})(H_2O)_2](NO_3)_2$ were prepared by a reported method.[57–59] $Cu(ClO_4)_2\cdot 6H_2O$ (Aldrich), ethylenediamine (Merck, India), triethylamine (Merck, India), and TBHP (Aldrich) were of reagent grade and used as received. Solvents such as MeCN (Merck India), methanol, ethanol, and others are of reagent grade and were dried by using standard methods before use.

Physical Measurements: Elemental analyses were performed with a Perkin–Elmer 240 elemental analyzer. ^1H NMR spectra were recorded with samples in $CDCl_3$ with a Bruker 300 MHz NMR spectrophotometer and tetramethylsilane (δ = 0 ppm) as an internal standard. Electronic spectra were recorded with an Agilent-8453 diode array UV/Vis spectrophotometer. Infrared spectra (400–

4000 cm^{-1}) were recorded from KBr pellets with a Nicolet Magna IR 750 series-II FTIR spectrophotometer.

Single-Crystal X-ray Diffraction: The single-crystal X-ray diffraction data of **1** and **2** were collected with a Bruker SMART APEX-II CCD diffractometer with graphite-monochromated Mo-K_α radiation (λ = 0.71073 Å). Data collection, reduction, structure solution, and refinement were performed by using the Bruker Apex-II suite (v2.0–2) software. All available reflections to $2\theta_{max}$ were harvested and corrected for Lorentz and polarization factors with Bruker SAINT plus. The reflections were then corrected for absorption, interframe scaling, and other systematic errors with SADABS.[60] The structures were solved by direct methods and refined by the full-matrix least-square technique based on F^2 with the SHELX-97 software package.[61] All non-hydrogen atoms were refined with anisotropic thermal parameters. All hydrogen atoms bound to carbon and nitrogen atoms were placed in their geometrically idealized positions, and hydrogen atoms bound to oxygen atoms of coordinated water molecules were found on the difference Fourier map; all of them were constrained to ride on their parent atoms. Drawings of molecules were generated with DIAMOND 3.0 and PLATON v1.6 software. The crystallographic data for **1** and **2** are listed in Table 5.

Table 5. Crystal data and Refinement parameters.

	1	**2**
Formula	$C_{30}H_{36}N_6O_{11}Cl_2Cu_2$	$C_{30}H_{34}N_6O_6ClCu_2$
Formula weight	854.65	737.18
Crystal system	monoclinic	triclinic
Space group	$P2_1/c$ (No. 14)	$P\bar{1}$ (No. 2)
a [Å]	10.7666(2)	8.351(2)
b [Å]	14.6661(4)	15.650(4)
c [Å]	22.1135(5)	23.231(5)
α [°]	90	89.482(5)
β [°]	92.202(2)	88.128(4)
γ [°]	90	87.402(5)
V [Å^3]	3489.23(14)	3031.3(12)
Z	4	4
D(calcd.) [Mg/m^3]	1.627	1.615
μ(Mo-K_α) [mm]	1.440	1.546
F(000)	1752	1516
Crystal size [mm]	0.20 × 0.25 × 0.30	0.25 × 0.28 × 0.30
Temperature [K]	293	100
Mo-K_α wavelength [Å]	0.71073	0.71073
θ min, max [°]	2.9, 27.00	1.3, 24.9
Data set	–13:13; –18:18; –28:28	–9:9; –18:18; –27:27
Total, unique data, R(int)	16293, 7621, 0.023	25049, 10518, 0.064
Observed data [$I > 2\sigma(I)$]	5474	7418
N_{ref}, N_{par}	7621, 467	10518, 823
R, wR_2, Goof	0.0277, 0.0831, 0.63	0.0769, 0.2025, 1.08

CCDC-914813 (for **1**) and -937186 (for **2**) contain the supplementary crystallographic data for this paper. These data can be obtained free of charge from The Cambridge Crystallographic Data Centre via www.ccdc.cam.ac.uk/data_request/cif.

Magnetic Measurements: The magnetic susceptibility measurements were obtained with the use of a Quantum Design superconducting quantum interference device (SQUID) magnetometer MPMS-XL. This magnetometer works between 1.8 and 300 K for dc applied fields of –7 to 7 T. Measurements were performed on polycrystalline samples of 11.63 mg for **1** and 25.47 mg for **2**. The magnetic data were corrected for the sample holder and diamagnetic contributions.

Experimental Set-up for Catalytic Oxidation: Liquid-phase oxidation reactions of styrene, cyclooctene, and norbornene were performed with **1** and **2** as catalysts and TBHP as oxidant. The overall reaction was performed in a two-necked round-bottomed flask fitted with a condenser and heated with a temperature-controlled oil bath on a magnetic stirrer. In a typical procedure, the substrate (0.5 mg) was dissolved with the same molar ratio of TBHP in acetonitrile (10 mL) containing the catalyst (0.02 mmol). The temperature of the reaction was maintained at 60 °C, and the products were collected at regular intervals. The progress of the reactions was monitored by an Agilent 7890D gas chromatograph (FID detector) fitted with a capillary column. The products were identified by comparison with known standards and confirmed by GC–MS with a Shimadzu-QP5050A GC–MS-E1 instrument.

2-Formyl-4-methyl-6-(3,5-dimethylpyrazole)phenol (HL): 2-Chloromethyl-6-formyl-4-methylphenol (1.515 g, 8.2 mmol) was dissolved in dry tetrahydrofuran (THF, 15 mL) in a round-bottomed flask. 3,5-Dimethylpyrazole (0.7883 g, 8.2 mmol) and triethylamine (Et_3N, 1.659 g, 16.4 mmol) were dissolved in dry THF (10 mL), and this mixture was added dropwise to the 2-chloromethyl-6-formyl-4-methylphenol solution. The instant precipitation of Et_3NHCl was observed and the solution turned bright yellow (Scheme 3). The solution was stirred for 24 h, and the precipitated Et_3NHCl was removed by filtration. The solvent (THF) was removed under reduced pressure to afford an oily product, which yielded a light yellow crystalline solid after a couple of days in a refrigerator. The solid product was then collected by filtration and washed with cold ether, yield 72%. ^1H NMR ($CDCl_3$, 300 MHz): δ = 2.23–2.28 (m, 9 H, $ArCH_3$), 5.27 (s, 2 H, CH_2), 7.09 (s, 1 H, ArH), 7.27 (s, 1 H, ArH), 7.28 (s, 1 H, ArH), 9.88 (s, 1 H, CHO), 11.23 (br s,1 H, ArOH) ppm.

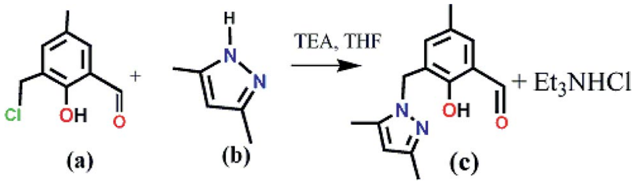

Scheme 3.

[$Cu^{II}_2(L)(H_2O)(ClO_4)_2$] (1): 2-Formyl-4-methyl-6-(3,5-dimethylpyrazole)phenol (0.244 mg, 1.00 mmol) and ethylenediamine (0.03 mg, 0.50 mmol) in methanol (30 mL) were heated to reflux for 40 min (Scheme 4). After the solution had cooled to room temperature, copper perchlorate hexahydrate (0.370 mg, 1.00 mmol) was added, and the mixture was heated to reflux for a further 60 min, whereupon the yellow solution turned green. The solution was filtered, and slow evaporation of the methanol yielded rod-shaped green crystals suitable for X-ray studies, yield 78%. $C_{30}H_{36}Cl_2Cu_2N_6O_{11}$ (854.65): calcd. C 42.12, H 4.21, N 9.83; found C 42.35, H 4.28, N 9.38. IR: $\tilde{\nu}$ = 1091 (ClO_4^-, coordinated), 1650 (C=N), 3429 (H_2O) cm^{-1}.

[$Cu^ICu^{II}(L)$](ClO_4) (2): 2-Formyl-4-methyl-6-(3,5-dimethylpyrazole)phenol (0.244 mg, 1.00 mmol) and ethylenediamine (0.03 mg, 0.50 mmol) in methanol (30 mL) were heated to reflux for 40 min. After the solution had cooled to room temperature, copper perchlorate hexahydrate (0.185 mg, 0.50 mmol) was added, and the mixture was heated to reflux for 1 hour. [Cu(2,2′-bipy)(H_2O)$_2$](NO_3)$_2$ (0.382 mg, 1.0 mmol) was then added, and the mixture was heated to reflux for another hour. The yellow solution turned green. The solution was filtered, and slow evaporation of the methanol yielded rod-shaped green crystals suitable for X-ray studies, yield 65%. $C_{30}H_{34}ClCu_2N_6O_6$ (737.18): calcd. C 48.88, H 4.65, N

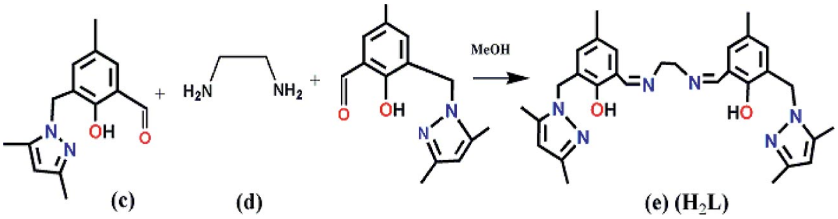

Scheme 4.

11.40; found C 48.35, H 4.78, N 11.38. IR: $\tilde{\nu}$ = 1096 (ClO_4^-, ionic), 1630 (C=N) cm^{-1}.

Supporting Information (see footnote on the first page of this article): Plot of conversion vs. time for epoxidation catalyzed by **2**, results of BVS calculations, plot of the field dependence of the magnetization of **2**.

Acknowledgments

Financial supports from Council of Scientific and Industrial Research (CSIR), New Delhi [01(2490)/11/EMR-II] is gratefully acknowledged. R. C., M. R., and I. B. thank the University of Bordeaux, the Centre National de la Recherche Scientifique (CNRS), and the Region Aquitaine for financial support and also the Erasmus Mundus Mobility with Asia program for the PhD fellowship of I. B.

---

[1] O. Kahn, *Molecular Magnetism*, VCH Publishers, New York, **1993**.

[2] K. D. Karlin, Z. Tyeklor (Eds.), *Bioorganic Chemistry of Copper*, Chapman & Hall, New York **1993**.

[3] K. A. Magnus, H. Ton-That, J. E. Carpenter, *Chem. Rev.* **1994**, *94*, 727–735.

[4] R. E. Stenkamp, *Chem. Rev.* **1994**, *94*, 715–726.

[5] E. I. Solomon, M. M. Sundaram, T. E. Machonkin, *Chem. Rev.* **1996**, *96*, 2563–2605.

[6] B. J. Wallar, J. D. Lipscomb, *Chem. Rev.* **1996**, *96*, 2625–2657.

[7] D. B. Brown (Ed.), *Mixed-Valence Compounds, Theory and Applications in Chemistry, Physics, Geology, and Biology*, Reidel, Boston, **1980**.

[8] E. I. Solomon in *Copper Proteins* (Ed.: T. G. Spiro), Wiley, New York, **1981**, Chap. 2 and references cited therein.

[9] a) S. Leininger, B. Olenyuk, P. J. Stang, *Chem. Rev.* **2000**, *100*, 853–907; b) R. D. Schnebeck, E. Freisinger, F. Glahe, B. Lippert, *J. Am. Chem. Soc.* **2000**, *122*, 1381–1390; c) S. S. Sun, A. J. Lees, *J. Am. Chem. Soc.* **2000**, *122*, 8956–8967.

[10] a) F. Würthner, A. Sautter, *Chem. Commun.* **2000**, 445–446; b) F. Würthner, A. Sautter, D. Schmid, P. J. A. Weber, *Chem. Eur. J.* **2001**, *7*, 894–902; c) K. D. Benkstein, J. T. Hupp, C. L. Stern, *Angew. Chem.* **2000**, *112*, 3013; *Angew. Chem. Int. Ed.* **2000**, *39*, 2891–2893; d) H. Hartmann, S. Berger, R. Winter, J. Fiedler, W. Kaim, *Inorg. Chem.* **2000**, *39*, 4977–4980.

[11] a) P. L. Jones, J. C. Jeffery, J. P. Maher, J. A. McCleverty, P. H. Rieger, M. D. Ward, *Inorg. Chem.* **1997**, *36*, 3088–3095; b) S. Zahn, J. W. Canary, *Science* **2000**, *288*, 1404–1407.

[12] a) W. Kaim, B. Schwederski, *Bioinorganic Chemistry: Inorganic Elements in the Chemistry of Life*, Wiley, Chichester, UK, **1995**; b) R. H. Holm, P. Kennepohl, E. I. Solomon, *Chem. Rev.* **1996**, *96*, 2239–2314.

[13] a) D. W. Randall, S. D. George, B. Hedman, K. D. Hodgson, K. Fujisawa, E. I. Solomon, *J. Am. Chem. Soc.* **2000**, *122*, 11620–11631; b) D. W. Randall, S. D. George, P. L. Holland, B. Hedman, K. O. Hodgson, W. B. Tolman, E. I. Solomon, *J. Am. Chem. Soc.* **2000**, *122*, 11632–11648; c) K. K. Nanda, A. W. Addison, R. J. Butcher, M. R. McDevitt, T. N. Rao, E. Sinn, *Inorg. Chem.* **1997**, *36*, 134–135; d) S. Knapp, T. P. Keenan, X. Zhang, R. Fikar, J. A. Potenza, H. J. Schugar, *J. Am. Chem. Soc.* **1990**, *112*, 3452–3464; e) P. L. Holland, W. B. Tolman, *J. Am. Chem. Soc.* **1999**, *121*, 7270–7271; f) N. Kitajima, K. Fujisawa, M. Tanaka, Y. Moro-oka, *J. Am. Chem. Soc.* **1992**, *114*, 9232–9233; g) P. L. Holland, W. B. Tolman, *J. Am. Chem. Soc.* **2000**, *122*, 6331–6332.

[14] a) M. B. Robin, P. Day, *Adv. Inorg. Chem. Radiochem.* **1968**, *10*, 247–422; b) H. Hartmann, S. Berger, R. Winter, J. Fiedler, W. Kaim, *Inorg. Chem.* **2000**, *39*, 4977–4980.

[15] a) G. Dong, C.-q. Qian, C.-y. Duan, K.-l. Pang, Q.-j. Meng, *Inorg. Chem.* **2003**, *42*, 2024–2030; b) G. Dong, Q. Chunqi, D. Chun-ying, P. Ke-liang, M. Qing-jin, *Inorg. Chem.* **2003**, *42*, 20242030; c) J.-i. Setsune, T. Yokoyama, S. Muraoka, H.-w. Huang, T. Sakurai, *Angew. Chem. Int. Ed.* **2000**, *39*, 1115–1117; *Angew. Chem.* **2000**, *112*, 1160–1162.

[16] a) T. K. Maji, D. Ghoshal, E. Zangrando, J. Ribas, N. R. Chaudhuri, *CrystEngComm* **2004**, *6*, 623–626; b) X.-M. Zhang, X.-M. Chen, *Eur. J. Inorg. Chem.* **2003**, *6*, 413–417; c) X. M. Zhang, Y. F. Zhao, H. S. Wu, S. R. Batten, S. W. Ng, *Dalton Trans.* **2006**, 3170–3178; d) J. He, J. X. Zhang, C. K. Tsang, Z. Xu, Y. G. Yin, D. Li, S. W. Ng, *Inorg. Chem.* **2008**, *47*, 7948–7950; e) M. L. Tong, L. J. Li, K. Mochizuki, H. C. Chang, X. M. Chen, Y. Li, S. Kitagawa, *Chem. Commun.* **2003**, 428–429; f) H. Zhao, Z. R. Qu, Q. Ye, X. S. Wang, J. Zhang, R. G. Xiong, X. Z. You, *Inorg. Chem.* **2004**, *43*, 1813–1815; g) J. Tao, Y. Zhang, M.-L. Tong, X. M. Chen, T. Yuen, C. L. Lin, X. Huang, J. Li, *Chem. Commun.* **2002**, 1342–1343; h) T. Okubo, R. Kawajiri, T. Mitani, T. Shimoda, *J. Am. Chem. Soc.* **2005**, *127*, 17598–17599; i) Y. Cai, Y. Wang, Y. Li, X. Wang, X. Xin, C. Liu, H. Zheng, *Inorg. Chem.* **2005**, *44*, 9128–9130; j) P. Mukherjee, M. G. B. Drew, M. Estrader, C. Diaz, A. Ghosh, *Inorg. Chim. Acta* **2008**, *361*, 161–172; k) S. Mohapatra, T. K. Maji, *Dalton Trans.* **2010**, *39*, 3412–3419.

[17] D. G. Lonnon, D. C. Craig, S. B. Colbran, *Inorg. Chem. Commun.* **2006**, *9*, 887–890.

[18] W. Zhang, J. L. Loebach, S. R. Wilson, E. N. Jacobsen, *J. Am. Chem. Soc.* **1990**, *112*, 2801–3803.

[19] R. I. Kureshy, N. H. Khan, S. H. R. Abdi, P. Iyer, A. K. Bhatt, *J. Mol. Catal. A* **1997**, *120*, 101–108.

[20] T. G. Traylor, R. Miksztal, *J. Am. Chem. Soc.* **1989**, *111*, 7443–7748.

[21] C. C. Franklin, R. B. VanAtta, A. F. Tai, J. S. Valentine, *J. Am. Chem. Soc.* **1984**, *106*, 814–816.

[22] A. F. Tai, L. D. Margerum, J. S. Valentine, *J. Am. Chem. Soc.* **1986**, *108*, 5006–5008.

[23] W. Nam, J. S. Valentine, *J. Am. Chem. Soc.* **1990**, *112*, 4977–4979.

[24] W. Yang, F. Diederichm, J. S. Valentine, *J. Am. Chem. Soc.* **1991**, *113*, 7195–7205.

[25] R. Krishna, S. Vancheesan, *J. Mol. Catal. A* **2000**, *157*, 15–24.

[26] C. Bousquet, D. G. Gilheany, *Tetrahedron Lett.* **1995**, *36*, 7739–7742.

[27] H. Imanishi, T. Katsuki, *Tetrahedron Lett.* **1997**, *38*, 251–254.

[28] R. I. Kureshy, N. H. Khan, S. H. R. Abdi, S. T. Patel, P. Iyer, *J. Mol. Catal. A* **1999**, *150*, 175–183.

[29] W. Yang, F. Diederich, J. S. Valentine, *J. Am. Chem. Soc.* **1990**, *112*, 7826–7828.

[30] T. Tanase, K. Mano, Y. Yamamoto, *Inorg. Chem.* **1993**, *32*, 3995–4003.

[31] a) S. Zolezzi, A. Decinti, E. Spodine, *Polyhedron* **1999**, *18*, 897–904; b) S. Rayati, S. Zakavi, M. Koliaei, A. Wojtczak, A. Kozakiewicz, *Inorg. Chem. Commun.* **2010**, *13*, 203–207; c) C. Adhikary, R. Bera, B. Dutta, S. Jana, G. Bocelli, A. Cantoni, S. Chaudhuri, S. Koner, *Polyhedron* **2008**, *27*, 1556–1562; d) R. Bera, C. Adhikary, S. Ianelli, S. Chaudhuri, S. Koner, *Polyhedron* **2010**, *29*, 2166–2170.

[32] S. Zolezzi, E. Spodine, A. Decinti, *Polyhedron* **2002**, *21*, 55–59.

[33] S. Zolezzi, E. Spodine, A. Decinti, *Polyhedron* **2003**, *22*, 1653–1658.

[34] S. Biswas, A. Dutta, K. K. Das, M. Ali, *Dalton Trans.* **2013**, DOI: 10.1039/c3dt51359a.

[35] J. Wang, M. L. Tong, *Acta Crystallogr., Sect. E* **2004**, *60*, m1223–m1224.

[36] a) D. H. Buisson, A. William, L. Dudeney, J. Irving, *J. Chem. Soc. Faraday Trans.* **1979**, *75*, 2496–2506; b) S. Kitagawa, M. Munakata, A. Higashie, *Inorg. Chim. Acta* **1984**, *84*, 79–84.

[37] S. Sundararajan, E. L. Wehry, *J. Inorg. Nucl. Chem.* **1972**, *34*, 3699–3709.

[38] S. Sundararajan, E. L. Wehry, *J. Phys. Chem.* **1972**, *76*, 1528–1536.

[39] F. H. Jardine, *Adv. Inorg. Chem. Radiochem.* **1975**, *17*, 115–163.

[40] G. A. Barclay, C. M. Harris, J. V. Kingstone, *Chem. Ind.* **1965**, 227.

[41] J. P. Naskar, S. Hati, D. Datta, *Acta Crystallogr., Sect. B* **1997**, *53*, 885–894.

[42] E. Movahedi, H. Golchoubian, *J. Mol. Struct.* **2006**, *787*, 167–171.

[43] J. S. Costa, C. M. Markus, I. Mutikainen, P. Gamez, J. Reedijk, *Inorg. Chim. Acta* **2010**, *363*, 2046–2050.

[44] S. Seelan, A. K. Sinha, D. Srinivas, S. Sivasanker, *J. Mol. Catal. A* **2000**, *157*, 163–171.

[45] P. Karandikar, M. Agashe, K. Vijayamohanan, A. Chandwadkar, *J. Appl. Catal. A* **2004**, *257*, 133–143.

[46] D. E. De Vos, M. Dams, B. F. Sels, P. A. Jacobs, *Chem. Rev.* **2002**, *102*, 3615–3640.

[47] T. Osako, S. Nagatomo, Y. Tachi, T. Kitagawa, S. Itoh, *Angew. Chem.* **2002**, *114*, 4501; *Angew. Chem. Int. Ed.* **2002**, *41*, 4325–4328.

[48] S. T. Prigge, B. A. Eipper, R. E. Mains, L. M. Amzel, *Science* **2004**, *304*, 864–867.

[49] R. A. Ghiladi, K. R. Hatwell, K. D. Karlin, H. W. Huang, P. Moënne-Loccoz, C. Krebs, B. H. Huynh, L. A. Marzilli, R. J. Cotter, S. Kaderli, A. D. Zuberbühler, *J. Am. Chem. Soc.* **2001**, *123*, 6183–6184.

[50] a) S. Jana, S. Bhunia, B. Dutta, S. Koner, *Appl. Catal. A* **2011**, *392*, 225–232; b) S. Jana, B. Dutta, R. Bera, S. Koner, *Langmuir* **2007**, *23*, 2492–2496.

[51] a) G. Das, R. Shukla, S. Mandal, R. Singh, P. K. Bharadwaj, *Inorg. Chem.* **1997**, *36*, 323–329; b) S. Bunce, R. J. Cross, L. J. Farrugia, S. Kunchandy, L. L. Meason, K. W. Muir, M. O'Donnell, R. D. Peacock, D. Stirling, S. J. Teat, *Polyhedron* **1998**, *17*, 4179–4187; c) S. Zolezzi, E. Spodine, A. Decinti, *Polyhedron* **2003**, *22*, 1653–1658; d) X. H. Lu, Q. H. Xia, H. J. Zhan, H. X. Yuan, C. P. Ye, K. X. Su, G. Xu, *J. Mol. Catal. A* **2006**, *250*, 62–69.

[52] D. Saha, T. Maity, T. Dey, S. Koner, *Polyhedron* **2012**, *35*, 55–61.

[53] J. H. van Vleck, *The Theory of Electric and Magnetic Susceptibility*, Oxford University Press, **1932**.

[54] K. Kambe, *J. Phys. Soc. Jpn.* **1950**, *5*, 48–51.

[55] C. J. O'Connor, *Prog. Inorg. Chem.* **1982**, *29*, 203–283.

[56] a) V. H. Crawford, H. W. Richardson, J. R. Wasson, D. J. Hodgson, W. E. Hatfield, *Inorg. Chem.* **1976**, *15*, 2107–2110; b) M. Andruh, *Chem. Commun.* **2007**, 2565–2577; c) A. M. Kirillov, Y. Y. Karabach, M. Haukka, M. F. C. Guedes da Silva, J. Sanchiz, M. N. Kopylovich, A. J. L. Pombeiro, *Inorg. Chem.* **2008**, *47*, 162–175; d) L. J. Farrugia, D. S. Middlemiss, R. Sillanpää, P. Seppälä, *J. Phys. Chem. A* **2008**, *112*, 9050–9067; e) P. Seppälä, E. Colacio, A. J. Mota, R. Sillanpää, *Inorg. Chim. Acta* **2010**, *363*, 755–762.

[57] E. Lambert, B. Chabut, S. C. Noblat, A. Deronzier, G. Chottard, A. Bousseksou, J. P. Tuchagues, J. Laugier, M. Bardet, J. M. Latour, *J. Am. Chem. Soc.* **1997**, *119*, 9424–9437.

[58] E. Garribba, G. Micera, D. Sanna, L. Strinna-Erre, *Inorg. Chim. Acta* **2000**, *299*, 253–261.

[59] I. Banerjee, P. N. Samanta, K. K. Das, R. Ababei, M. Kalisz, A. Girard, C. Mathonière, Y. G. Li, M. Nethaji, R. Clérac, M. Ali, *Dalton Trans.* **2013**, *42*, 1879–1892.

[60] G. M. Sheldrick, *SAINT* (version 6.02), *SADABS* (version 2.03), Bruker AXS Inc., Madison, Wisconsin, **2002**.

[61] a) G. M. Sheldrick, *Acta Crystallogr., Sect. A* **2008**, *64*, 112–122; b) G. M. Sheldrick, *SHELXL-97*, *Crystal Structure Refinement Program*, University of Göttingen, Germany, **1997**.

Received: May 3, 2013

Dinuclear Complexes

S. Biswas, A. Dutta, M. Dolai, I. Bhowmick, M. Rouzières, H. M. Lee, R. Clérac, M. Ali* 1–10

Dinuclear Cu^{II}–Cu^{II} and Cu^{I}–Cu^{II} Complexes of a Compartmental Ligand – Syntheses, Structures, Magnetic, and Catalytic Studies

Keywords: Schiff bases / Copper / Structure elucidation / Magnetic properties / Epoxidation

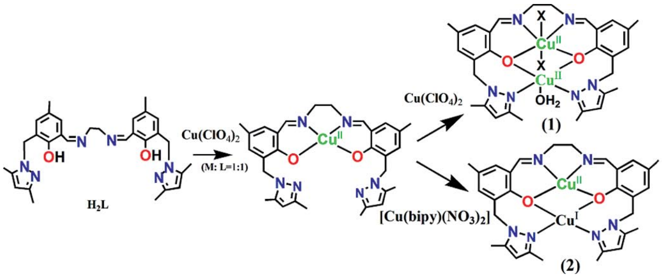

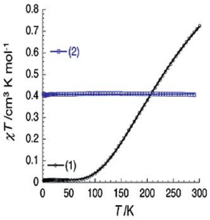

Dinuclear Cu^{II}–Cu^{II} (**1**) and Cu^{I}–Cu^{II} (**2**) complexes derived from a new N_4O_2 donor ligand (H_2L) are synthesized and characterized by single-crystal X-ray diffraction, UV/Vis spectroscopy, and magnetic measurements. In **1**, there is strong antiferromagnetic coupling between the Cu atoms. In **2**, the Cu^{I} ion is diamagnetic and the remaining $S = 1/2$ Cu^{II} magnetic center follows a Curie law with $g = 2.06(5)$.